Published in final edited form as:
J Neuropathol Exp Neurol. 2008 December ; 67(12): 1194–1204. doi:10.1097/NEN.0b013e31818fbe1e.

Gene Expression Profiling of NF1-Associated and Sporadic Pilocytic Astrocytoma Identifies Aldehyde Dehydrogenase 1 Family, Member L1 (ALDH1L1) as an Underexpressed Candidate Biomarker in Aggressive Subtypes

Fausto J. Rodriguez, MD[1], **Caterina Giannini, MD, PhD**[1], **Yan W. Asmann, PhD**[3], **Mukesh K. Sharma, PhD**[2], **Arie Perry, MD**[4], **Kathleen M. Tibbetts, BS**[2], **Robert B. Jenkins, MD, PhD**[1], **Bernd W. Scheithauer, MD**[1], **Shrikant Anant, PhD**[5], **Sarah Jenkins, MS**[6], **Charles G. Eberhart, MD, PhD**[7], **Jann N. Sarkaria, MD**[8], and **David H. Gutmann, MD, PhD**[2]

[1]Department of Laboratory Medicine and Pathology, Mayo Clinic Rochester, Minnesota. [2]Department of Neurology, Washington University School of Medicine, St. Louis, Missouri. [3]Division of Biomedical Informatics, Mayo Clinic Rochester, Minnesota. [4]Division of Neuropathology, Washington University School of Medicine, St. Louis, Missouri. [5]University of Oklahoma Health Sciences Center, Oklahoma City, Oklahoma. [6]Biostatistics, Mayo Clinic Rochester, Minnesota. [7]Department of Pathology, Johns Hopkins Medical Institutions, Baltimore, Maryland. [8]Radiation Oncology, Mayo Clinic Rochester, Minnesota.

Abstract

Pilocytic astrocytomas (PAs) are WHO grade I gliomas; they most often affect children and young adults and occur in patients with neurofibromatosis type 1 (NF-1). To identify genes that are differentially expressed in sporadic (S-PA) versus NF-1-associated PAs (NF1-PAs) and those that might reflect differences in clinical behavior, we performed gene expression profiling using Affymetrix U133 Plus2.0 GeneChip arrays in 36 S-PAs and 11 NF1-PAs. Thirteen genes were over-expressed and another 13 genes were under-expressed in NF1-associated PAs relative to S-PAs. Immunohistochemical studies performed on 103 tumors, representing 2 independently generated tissue microarrays, confirmed the differential expression of CUGBP2 ($p = 0.0014$), RANBP9 ($p = 0.0075$), ITGAV1 ($p = 0.0001$), and INFGR1 ($p = 0.024$) proteins. One of the underexpressed genes, aldehyde dehydrogenase 1 family, member L1 (*ALDH1L1*), was also reduced in clinically aggressive compared to typical PAs ($p = 0.01$) and in PAs with increased cellularity and necrosis. Furthermore, in an additional independent set of tumors, weak to absent ALDH1L1 expression was found in 13/18 (72%) clinically aggressive PAs, in 8/9 (89%) PAs with pilomyxoid features, in 7/10 (70%) PAs with anaplastic transformation and in 16/21 (76%) diffusely infiltrating astrocytomas of various grades. In summary, we have identified a molecular signature that distinguishes NF1-PA from S-PA, and found that *ALDH1L1* underexpression is associated with aggressive histology and/or biological behavior.

Keywords

Brain tumor; Glioma; Microarray; Molecular signature; Neurofibromatosis; Pilocytic astrocytoma

Correspondence and reprint requests to: Fausto J. Rodriguez, MD, Department of Laboratory Medicine and Pathology, Mayo Clinic, 200 1st St. SW, Rochester, MN 55905. Telephone: 507-538-9774; Fax: 507-284-1599. E-mail: Rodriguez.fausto@mayo.edu.

INTRODUCTION

Pilocytic astrocytomas (PAs) are WHO grade I tumors that typically affect children and young adults. These glial neoplasms represent the most common primary brain tumor in children, with an incidence of 0.87 per 100,000 individuals under 19 years of age (1). Most PAs arise in the cerebellum (2), but they also develop in the optic pathway, hypothalamic region, cerebral hemispheres, basal ganglia, brainstem, and spinal cord. Microscopically, PAs contain elongate bipolar astrocytes within a biphasic architecture consisting of compact Rosenthal fiber-rich areas, alternating with loose microcystic tissue associated with granular bodies and hyaline droplets (3). PAs often additionally have macrocysts and hyalinized vessels. In contrast to more aggressive glial neoplasms, PAs usually have rare to absent mitotic activity and low proliferative indices (4).

Patients with PAs generally have favorable outcomes, with 5-year overall survival rates of 96% following surgical intervention alone (5); however, a subset may progress and cause significant morbidity or mortality, despite lack of atypical histologic features (6). Conversely, increased proliferation, invasive growth pattern, and/or necrosis do not always predict aggressive behavior (7–9). In this regard, a recently described rare variant of PA, the pilomyxoid astrocytoma, is prone to more aggressive behavior, including cerebrospinal fluid dissemination and increased mortality(10). Therefore, under the current WHO classification pilomyxoid astrocytoma is assigned a grade II (11).

While most PAs arise in individuals without a known family history of astrocytoma, 15% of all PAs develop in individuals with the inherited tumor predisposition syndrome neurofibromatosis type 1 (NF1). In contrast to their sporadic counterparts, NF1-associated PAs typically occur in the optic pathway, and less frequently in the brainstem and other regions. Moreover, the majority of PAs arising in the setting of NF1 exhibit clinical behavior that is generally more favorable than that observed in individuals with sporadic PAs (9,11,12). This is particularly true of PAs that involve the optic pathway and which have occasionally been reported to regress spontaneously (12). To gain insight into the molecular differences between NF1-associated (NF1-PA) and sporadic (S-PA) PA, gene expression profiling studies have identified molecular signatures that distinguished these 2 subsets of PA (13,14). Molecular signatures that separate aggressive from typical PA, however, were not identified in these studies.

Since there are no pathologic features that accurately predict the clinical behavior of PAs, the discovery of molecular signatures that could stratify PAs by their clinical behavior would be of both prognostic and therapeutic importance. Specifically, there is a great need to identify molecular biomarkers that mark clinically aggressive PAs. One previous study suggested an association between PA MIB1 (Ki67) labeling index and decreased progression-free survival (6); however, this was not confirmed in other studies (15,16). Similarly, investigators have identified myelin basic protein as a potential marker underexpressed in subtotally resected PA that subsequently progress (17,18). Unfortunately, this finding was also not replicated in other studies(14).

In the present study, we sought to identify genes that might be associated with aggressive PA clinical behavior. We first performed high throughput gene expression profiling to identify molecular signatures that distinguish NF1-PA compared to S-PA. We next used this information to identify and validate aldehyde dehydrogenase 1 family, member L1 (*ALDH1L1*) as a differentially expressed gene that is underexpressed in more clinically aggressive astrocytoma subtypes.

MATERIALS AND METHODS

Patients and Tumor Samples

Tumors were classified as either "NF1-associated" using previously established clinical criteria (19) or "sporadic" when they occurred in patients without NF1 or other known glioma predisposition syndrome. PAs were termed "clinically-aggressive" if they recurred after gross total resection or displayed significant growth during therapy, irrespective of NF1 status. All studies were approved by the Institutional Review Boards at Mayo Clinic and Washington University.

Four sets of clinical tumor samples were used. First, 41 tumors previously subjected to microarray gene expression analyses, including 5 NF1-PAs, 36 S-PAs and 6 clinically aggressive PAs, were employed (14). Second, frozen samples from 6 NF1-PAs (1 considered clinically aggressive) were used for gene expression microarray analyses and 10 S-PAs (5 clinically aggressive, 5 typical) were used for quantitative real time RT-PCR (qRT-PCR). Third, 2 independently generated tissue microarrays (TMAs) containing samples from 103 patients (F = 56, M = 47, NF1-associated = 15, sporadic = 88) were employed for independent validation by immunohistochemistry. The median age at PA diagnosis in this group was 11 years (range 1–58 years). Tumor locations included optic pathways (13%), supratentorial CNS (26%), infratentorial CNS (59%), and site indeterminate (2%). Finally, a set of mostly sporadic tumors, including clinically aggressive PAs (n = 18), pilomyxoid astrocytomas (n = 9), PAs with anaplastic change (n = 10), diffusely infiltrating astrocytomas grades II–IV (n = 21), and non-neoplastic gliosis controls (n = 3) were used for secondary validation. In addition, 13 heterotopic glioblastoma xenografts grown in mouse flanks were used for conventional and qRT-PCR.

Microarray Analysis of Gene Expression

Tumor tissue was homogenized and total RNA extracted using TRIzol (Invitrogen, Carlsbad, CA) followed by QIAGEN RNeasy kit (QIAGEN, Inc., Valencia CA) purification, according to the manufacturer's recommendations. RNA quality was assessed using the Agilent 2100 bioanalyzer (Agilent Technologies, Palo Alto, CA). Double-stranded cDNA followed by cRNA synthesis and biotinylation were performed according to the GeneChip Expression Analysis Technical Manual (Affymetrix, Santa Clara, CA), followed by hybridization to Affymetrix HG-U133 Plus2.0 GeneChip arrays and data processing.

Raw CEL files were pre-processed using the GC-RMA algorithm (background subtraction, normalization, and expression summarization) and GeneSpring (Agilent Technologies). Comparisons were performed using the Student *t*-test, followed by pathway analyses with Ingenuity software (Ingenuity Systems, Redwood City, CA). False discovery rate was calculated as an additional threshold using the Benjamini and Hochberg method. To adjust for differential expression based on *NF1*-deficiency and tumor location, the genes in the final list were compared to a database of gene expression ratios (murine *Nf1*−/− astrocytes/wild-type astrocytes and human cortex/cerebellum glia, respectively) as previously described (14). The latter was obtained from Human U133A GeneChip microarray datasets from the GeneAtlas Project at the Genomics Institute of the Novartis Research Foundation.

Real Time RT-PCR

Quantitative analyses of gene expression were performed using TaqMan gene expression assays (Applied Biosystems, Foster City, CA). All probes contain a FAM reporter dye at the 5' end of the MGB probe and a non-fluorescent quencher at the 3' end. Predesigned gene expression assays for *ALDH1L1*, *SOX8*, and *CDGAP* (catalog numbers Hs01003850, Hs00232723, and Hs00393361 respectively) were used. Glyceraldehyde-3-phosphate

dehydrogenase (GAPDH) served as an internal control. A total of 1 μg of RNA was converted into cDNA, and 50 nanograms were loaded per well. All tumor samples were run in triplicate in an ABI 7900HT Fast Real-Time PCR system (Applied Biosystems) on 96-well plates. PCR reactions without cDNA were used as negative controls.

Data were analyzed using SDS software after converting the fluorescent data into cycle threshold (*C*t) measurements. The ΔΔCt calculations were employed to calculate fold changes. Further details about these analytic methods can be found at the Applied Biosystems website (www.appliedbiosystems.com).

Immunohistochemistry

The top differentially expressed genes, based on fold expression, statistical analysis, and availability of suitable antibodies, were confirmed by immunohistochemistry in additional PA sets obtained from the 2 tissue microarrays described above. Immunohistochemical stains were performed using a DAKO Autostainer (Dako North America, Inc., Carpinteria, CA) with the Dual Link Envision+ (Dako) detection system; EDTA or citrate (FOXO3A) were used for antigen retrieval. Diaminobenzidine (DAB) was the chromogen. All commercially available antibodies that worked in formalin-fixed paraffin-embedded tissue, as well as 2 previously tested antibodies (to CUGBP2 and PIM3) in different studies, were obtained. Information about the antibodies used is summarized in Table 1. ALDH1L1 immunohistochemistry was also performed on 5-μm full tissue sections on an additional independent dataset enriched for aggressive histologic subtypes.

Immunohistochemistry Scoring

Immunohistochemistry scoring was performed by a single neuropathologist (CG) on TMA sections or two neuropathologists (CG, FJR) on tissue sections in a blinded fashion, using a two-tiered scale (i.e. 0 = negative/minimal, 1 = positive). The median of several measurements from scoreable tissue microarray cores or whole tissue sections was used to obtain a final summary score for statistical analyses. Since the cellular localization of CUGBP2, FOXO3A and RANBP9 is nuclear, in addition to cytoplasmic, this intracellular localization was also noted. Quantitative evaluation of MIB-1 labeling indices was performed using the Hamamatsu NanoZoomer Digital Pathology for scanning images and IHCScore software for computer-assisted analyses (Bacus Laboratories, Inc., Bellingham, WA).

Statistical Methods

Patient and tumor characteristics were described using frequencies, medians, ranges and interquartile ranges as appropriate. Recurrence-free survival was illustrated using Kaplan-Meier survival curves and analyzed with Cox proportional hazard regression. The association between immunohistochemical scores from the TMA sets and several clinicopathologic features, including clinical aggressiveness, histologic atypia, necrosis, cellularity, mitotic activity, and MIB-1 labeling index, was evaluated with logistic or linear regression analyses adjusting by NF1 status and location, (i.e. optic pathway, supratentorial, infratentorial). The associations between immunohistochemical scores and NF1 status were adjusted by location. The Chi square or Fisher exact tests were used to compare proportions, and the Student *t* or Wilcoxon rank sum tests were used to compare continuous variables between the groups of interest. The Kappa statistic was used to calculate interobserver agreement for the second part of the immunohistochemical analysis. Statistical analyses were performed using SAS version 9 software (SAS Institute, Inc., Cary, NC).

RESULTS

Gene Expression Profiling of NF1-Associated and Sporadic PA

Student *t*-test identified 7,516 differentially expressed genes between sporadic tumors compared to those from patients with NF1 ($p < 0.05$). There were 191 transcripts with false discovery rate < 0.05 (Supplementary Table 1). Several genes in this list (e.g. *CUGBP* and *OBFC1*) were evaluated and/or validated by qRT-PCR in our previous study of PA (14). Genes with low or absent expression (means in both groups < 200) were excluded and the list was narrowed to a total of 61 genes. After excluding genes differentially expressed in *Nf1*-deficient primary murine astrocytes and tumor location, 13 genes were found to be overexpressed in NF1-PA and an additional 13 genes were underexpressed in NF1-PA relative to S-PA tumors (Fig. 1). To determine whether these genes were differentially expressed in other NF1-associated neoplasms, the list was compared to our prior dataset of gene expression profiles obtained with a U95Av2 chip of malignant peripheral nerve sheath tumors (MPNSTs)(20). The dataset included 13 (of 26) genes in the PA list that were not differentially expressed between NF1-associated and sporadic MPNSTs (Supplementary Fig. 1). These findings suggest that the NF1-PA gene expression signature is specific to PA and does not reflect NF1-associated tumorigenesis in general.

Validation of NF1-Associated PA Gene Expression Signature

Differentially expressed genes in the final list of 26 genes were validated by immunohistochemistry using two independently generated TMAs (Table 2). Logistic regression analyses adjusting for tumor location confirmed differences in expression between NF1-PA and S-PA for *CUGBP2* ($p = 0.0014$), *RANBP9* ($p = 0.0075$), *ITGAV* ($p = 0.0001$), *INFGR1* ($p = 0.024$), and *ABI1* ($p = 0.0584$). Representative images are shown in Figure 2. Because prior studies have shown that CUGBP2 regulates COX2 levels in breast carcinoma (21) we also performed COX2 immunohistochemistry and found no significant associations with NF1 status, clinical behavior, or CUGBP2 expression ($p > 0.05$)(data not shown). Analyses of the remaining immunohistochemistry results with relevant clinicopathologic parameters revealed an association between infiltration of the underlying parenchyma (as demonstrated by neurofilament protein positive axons) and immunostaining for CUGBP2 (strong nuclear, $p = 0.033$), IFNGR1 (cytoplasmic, $p = 0.032$), and FOXO3A (nuclear vs. negative/cytoplasmic, $p = 0.016$) after adjusting for location and NF1 status with logistic regression methods. SERPINA5 immunoreactivity was also associated with non-optic pathway tumor locations ($p = 0.0076$).

Differential Gene Expression in Aggressive PA

Although hierarchical clustering did not reveal any overall differences in gene expression between clinically aggressive and typical PA for the entire dataset or for the set of genes that were differentially expressed in NF1-PAs versus S-PAs (Fig. 3), *ALDH1L1*, *CDGAP*, and *SOX8*, were significantly determined to be underexpressed in the aggressive subgroup ($n = 7$) compared to typical PAs ($n = 40$) ($p = 0.019$, $p = 0.04$ and $p = 0.038$ respectively, Wilcoxon Rank-Sum Test) (Fig. 4a; Table 3).

To confirm these findings, we performed qRT-PCR on an independent set of sporadic PAs (5 aggressive, 5 typical) and 4 heterotopic glioblastoma xenografts. This analysis demonstrated a stepwise decrease in *ALDH1L1* relative expression in the three groups ($p = 0.0072$) (Fig. 4b). In these experiments, *ALDH1L1* was underexpressed by 3.7-fold in aggressive PAs samples compared to typical PAs, although this difference did not reach statistical significance ($p = 0.0758$, Wilcoxon Rank-Sum). In contrast, no differences in gene expression were noted between aggressive and typical PAs for *CDGAP* ($p = 0.46$) or *SOX8* ($p = 0.60$) (data not shown).

ALDH1L1 expression was next evaluated by immunohistochemistry. Reactive astrocytes in gliosis controls were strongly labeled for ALDH1L1, whereas neurons and vessels were negative (Fig. 5A). ALDH1L1 expression was decreased in aggressive versus typical PAs (5/7 vs. 11/46) ($p = 0.0097$)(Fig. 5B–F), and in those with increased cellularity (10/21 vs 3/18) ($p = 0.049$), necrosis (3/4 vs. 15/52) ($p = 0.048$) and elevated mitotic activity (12/24 vs. 6/30) ($p = 0.051$), after adjusting for tumor location and NF1 status with regression analyses. There was also a modest correlation between decreased ALDH1L1 staining and high MIB-1 labeling indices, which did not reach statistical significance ($p = 0.0816$). ALDH1L1 expression was not associated with NF1 status or location ($p > 0.05$). Kaplan Meier plot and Cox proportional hazards modeling demonstrated decreased recurrence-free survival in ALDH1L1 negative/minimally reactive tumors compared to immunopositive tumors ($p = 0.01$)(Fig. 6). These findings suggest that decreased ALDH1L1 protein expression is associated with aggressive histologic features and biologic behavior in PAs independent of NF1 status.

ALDH1L1 Expression in Aggressive Astrocytoma Subtypes

ALDH1L1 immunoexpression was also decreased in an additional independent tumor set enriched for clinically and histologically aggressive glial cell tumors, including rare PA variants (pilomyxoid astrocytoma and PA with anaplastic transformation) and diffusely infiltrating astrocytomas of grades II–IV (Fig. 5, Fig. 7a; Table 4). These tumors were scored by 2 independent observers. The concordance rate between the 2 observers was 0.73 and the kappa statistic 0. 47, which is consistent with moderate agreement. Most disagreements were secondary to difficulties in separating focal partial positivity from negative staining. The pattern of staining was heterogeneous. In particular, ALDH1L1 was under-expressed in cellular, more poorly differentiated areas of anaplastic and recurrent astrocytomas (Fig. 5). To extend these observations, conventional RT-PCR was performed on a set of heterotopic glioblastoma xenografts using primers that recognize human *ALDH1L1* mRNA. Because ALDH1L1 is strongly expressed in reactive astrocytes (Fig. 5a), we assessed mRNA expression in heterotopic glioblastoma xenografts as a pure human tumor cell population, and gliotic human brain samples that were rich in reactive astrocytes, as controls. *ALDH1L1* was under-expressed in 11 of 13 (87%) glioblastoma xenograft samples compared to 1/9 (13%) gliosis control specimens ($p = 0.0005$, Fisher exact test) (Fig. 7b). Human *ALDH1L1* was confirmed by sequencing of the PCR product in 3 of the positive cases (2 controls, 1 xenograft; data not shown). Collectively, these results implicate reduced ALDH1L1 expression in clinically- and histologically aggressive glial cell tumors.

DISCUSSION

Although our knowledge of the biology of diffusely infiltrating gliomas has increased significantly over the past decade, this is not the case for PAs. Molecular studies of PAs have traditionally proven difficult, in part because gross genetic abnormalities are usually absent. Conventional cytogenetic studies have usually demonstrated a normal diploid karyotype with chromosomal gains (typically involving chromosomes 7 and 8) occurring in approximately one third of the cases (22). For this reason, recent studies have highlighted the need to use higher resolution platforms to identify genomic aberrations in these tumors (23,24). Using these microarray analyses, two genes have been identified on chromosome 7 (23,25,26): homeodomain interacting protein kinase 2 (*HIPK2*) and v-raf murine sarcoma viral oncogene homolog B1 (*BRAF*), and another on chromosome 8 (27), Matrilin 2 (*MATN2*), which may play important roles in low-grade glioma pathogenesis and clinical behavior. In this regard, *HIPK2* and *BRAF* overexpression can promote cell growth (23,28), while *MATN2* overexpression was observed in sporadic PAs with clinically aggressive behavior (27).

PA tumors can develop sporadically or in the context of the NF1 inherited tumor predisposition syndrome. Previous studies by our group and others have identified molecular genetic differences between NF1-PAs and S-PAs that may be relevant to the clinical behavior of these tumors. For example, loss of heterozygosity at the *NF1* locus is almost universal in NF1-PA but is not observed in S-PA(29). In this regard, NF1-PAs are characterized by loss of *NF1* gene expression, whereas other genetic events that increase cell growth must underlie the genesis of S-PAs. We previously showed that *Nf1* inactivation in murine astrocytes results in the selective hyperactivation of KRAS (30). Based on this observation, we sequenced sporadic PAs for activating mutations in *KRAS* and identified one such mutation in an S-PA (31). A subsequent study also identified a *KRAS* mutation in a S-PA(32) but *KRAS* mutation is a rare event in S-PAs, suggesting that other genetic events are important for the pathogenesis and continued growth of these common brain tumors.

Previous studies using high throughput gene expression profiling have identified gene expression patterns unique to NF1-PAs that distinguish these tumors from their sporadic counterparts (13,14). Here, we have extended gene expression profiling using a larger set of NF1-PAs than previous studies (n = 11) to identify clinically relevant markers in PAs, and made several observations. First, while prior studies have only identified overexpressed genes in NF1-PAs compared to S-PAs, we identified several differentially expressed genes that were either overexpressed or underexpressed in NF1-PA compared to S-PA. Second, we validated the NF1-PA molecular signature at the protein level using a large number of clinically annotated samples. Third, we identified ALDH1L1 as an underexpressed transcript in aggressive PAs, independent of NF1 status.

We validated the differential expression of *CUGBP2*, *RANBP9*, *INFGR1* and *ITGAV* in NF1-PA compared to S-PA. These transcripts may be biologically relevant since CUGBP2 binds to the 3' untranslated region of certain mRNAs, including *COX2*, and may affect their stability. This interaction has been previously explored in breast (21) and colon cancer (33). In the present study, we did not identify a relationship between *CUGBP2* and *COX2* expression, raising the possibility that *CUGBP2* may have an alternative mechanism of action in PAs. *ITGAV* encodes the integrin alpha$_v$ chain, which can mediate interactions with the extracellular matrix and facilitate signal transduction. *ITGAV* expression has prognostic importance in ovarian carcinoma (34), melanoma (35) and head and neck cancer (36). For example, the identification of polymorphisms in microRNA-binding sites for integrin genes have suggested that certain integrin alleles predict worse survival in patients with breast cancer (37) and susceptibility to hepatocellular carcinoma (38). RANBP9 belongs to the RAS superfamily, and is a GTP binding protein that interacts with the proto-oncogene MET (39) as well as HIPK2 (40). This association is intriguing, based on our recent finding that *HIPK2* expression is increased in PA (23). It is also worth noting that RANBP9, through its interaction with MET, modulates Ras/Erk signaling, a pathway regulated by the NF1 protein, neurofibromin (39). Further studies of these proteins, including pathway analyses and functional characterization, will be necessary to define their specific roles in the pathogenesis of NF1-PA.

The identification of biomarkers that identify clinically aggressive PA has proven to be challenging. Although we did not find a gene expression signature that separates aggressive and typical PA subtypes, we identified *ALDH1L1*, *FTHFD* as an underexpressed gene in aggressive subtypes. ALDH1L1 is an enzyme involved in folate metabolism that catalyzes the conversion of 10-formyltetrahydrofolate (10-FTHF) to tetrahydrofolate, and may play a regulatory role in cell proliferation (41). A recent study has demonstrated this enzyme to be developmentally-regulated in the neural tube (42), where its expression correlates with decreased cellular proliferation. In a recent gene expression profile study of carefully isolated CNS cell types, Cahoy and colleagues identified ALDH1L1 as a specific astrocyte marker,

more widely expressed in the brain than GFAP (43). Collectively, these findings suggest that ALDH1L1 is important in both brain development and astrocyte biology.

While the precise role of ALDH1L1 in the CNS is not known, *ALDH1L1* has been reported to be underexpressed in cancer and to stimulate apoptosis when it is overexpressed in vitro (44). We confirmed *ALDH1L1* under-expression at the mRNA and protein levels and suggest that this under-expression may be associated with more aggressive astrocytoma clinical behavior. It is worth noting that one property of ALDH1L1 involves depletion of 10-FTHF, which is required for *de novo* purine biosynthesis (44). Since antifolate compounds that inhibit enzymes involved in these reactions show antitumor effects (45,46), it is possible that these compounds may have particular utility in targeting ALDH1L1-deficient astrocytomas. Detailed functional studies of ALDH1L1 in experimental glioma model systems will be required to define the role of this gene in astrocytoma clinical behavior.

In summary, we performed a detailed analysis of gene expression of NF1-PAs and S-PAs and validated the differential expression of several of the genes that form a specific molecular NF1-associated PA molecular signature. In addition, we identified ALDH1L1 as an underexpressed biomarker of tumor aggressiveness in astrocytic tumors. Additional retrospective and prospective studies examining this potential biomarker are necessary to demonstrate its ultimate clinical utility.

Supplementary Material

Refer to Web version on PubMed Central for supplementary material.

ACKNOWLEDGMENTS

This work was supported in part by NIH training grant T32 NS07494-04 (FJR), grant 31170 from the Department of Laboratory Medicine and Pathology, Mayo Clinic (FJR, CG), Schnuck Markets, Inc. (DHG), and Mayo SPORE in Brain Cancer, P50 CA108961 (CG, RBJ, JNS).

The authors thank the Microarray, Tissue and Cell Molecular Analysis Shared Resources of the Mayo Clinic for excellent technical assistance as well as Professor Naofumi Mukaida at Kanazawa University, Japan, for kindly sharing PIM-3 antibody for immunohistochemical studies. We also appreciate the technical assistance of Mr. Ryan Emnett and data analysis by Ms. Jane Kahl.

REFERENCES

1. CBTRUS. Primary Brain Tumors in the United States, 2000–2004. Hinsdale, IL: Central Brain Tumor Registry of the United States; 2008.
2. Burkhard C, Di Patre PL, Schuler D, et al. A population-based study of the incidence and survival rates in patients with pilocytic astrocytoma. J Neurosurg 2003;98:1170–1174. [PubMed: 12816259]
3. Scheithauer, B.; Hawkins, C.; Tihan, T., et al. Pilocytic Astrocytoma. In: Louis, DN.; Ohgaki, H.; Wiestler, O.; Cavenee, W., editors. WHO Classification of Tumours of the Central Nervous System. Vol. 4th ed.. Lyon: International Agency for Research on Cancer; 2007. p. 14-21.
4. Giannini C, Scheithauer BW, Burger PC, et al. Cellular proliferation in pilocytic and diffuse astrocytomas. J Neuropathol Exp Neurol 1999;58:46–53. [PubMed: 10068313]
5. Ohgaki H, Kleihues P. Population-based studies on incidence, survival rates, and genetic alterations in astrocytic and oligodendroglial gliomas. J Neuropathol Exp Neurol 2005;64:479–489. [PubMed: 15977639]
6. Bowers DC, Gargan L, Kapur P, et al. Study of the MIB-1 labeling index as a predictor of tumor progression in pilocytic astrocytomas in children and adolescents. J Clin Oncol 2003;21:2968–2973. [PubMed: 12885817]

7. Forsyth PA, Shaw EG, Scheithauer BW, et al. Supratentorial pilocytic astrocytomas. A clinicopathologic, prognostic, and flow cytometric study of 51 patients. Cancer 1993;72:1335–1342. [PubMed: 8339223]
8. Machen SK, Prayson RA. Cyclin D1 and MIB-1 immunohistochemistry in pilocytic astrocytomas: a study of 48 cases. Hum Pathol 1998;29:1511–1516. [PubMed: 9865840]
9. Rodriguez FJ, Perry A, Gutmann DH, et al. Gliomas in neurofibromatosis type 1: A clinicopathologic study of 100 patients. J Neuropathol Exp Neurol 2008;67:240–249. [PubMed: 18344915]
10. Tihan T, Fisher PG, Kepner JL, et al. Pediatric astrocytomas with monomorphous pilomyxoid features and a less favorable outcome. J Neuropathol Exp Neurol 1999;58:1061–1068. [PubMed: 10515229]
11. Louis, D.; Ohgaki, H.; Wiestler, O., et al. WHO Classification of Tumours of the Central Nervous System. Vol. 4th ed.. Lyon, France: IARC press; 2007.
12. Parsa CF, Hoyt CS, Lesser RL, et al. Spontaneous regression of optic gliomas: thirteen cases documented by serial neuroimaging. Arch Ophthalmol 2001;119:516–529. [PubMed: 11296017]
13. Gutmann DH, Hedrick NM, Li J, et al. Comparative gene expression profile analysis of neurofibromatosis 1-associated and sporadic pilocytic astrocytomas. Cancer Res 2002;62:2085–2091. [PubMed: 11929829]
14. Sharma MK, Mansur DB, Reifenberger G, et al. Distinct genetic signatures among pilocytic astrocytomas relate to their brain region origin. Cancer Res 2007;67:890–900. [PubMed: 17283119]
15. Fisher BJ, Naumova E, Leighton CC, et al. Ki-67: A prognostic factor for low-grade glioma? Int J Radiat Oncol Biol Phys 2002;52(4):996–1001. [PubMed: 11958894]
16. Dirven CM, Koudstaal J, Mooij JJ, et al. The proliferative potential of the pilocytic astrocytoma: the relation between MIB-1 labeling and clinical and neuro-radiological follow-up. J Neurooncol 1998;37:9–16. [PubMed: 9525833]
17. Wong KK, Chang YM, Tsang YT, et al. Expression analysis of juvenile pilocytic astrocytomas by oligonucleotide microarray reveals two potential subgroups. Cancer Res 2005;65:76–84. [PubMed: 15665281]
18. Takei H, Yogeswaren ST, Wong KK, et al. Expression of oligodendroglial differentiation markers in pilocytic astrocytomas identifies two clinical subsets and shows a significant correlation with proliferation index and progression free survival. J Neurooncol 2008;86:183–190. [PubMed: 17690840]
19. Gutmann DH, Aylsworth A, Carey JC, et al. The diagnostic evaluation and multidisciplinary management of neurofibromatosis 1 and neurofibromatosis 2. JAMA 1997;278:51–57. [PubMed: 9207339]
20. Watson MA, Perry A, Tihan T, et al. Gene expression profiling reveals unique molecular subtypes of Neurofibromatosis Type I-associated and sporadic malignant peripheral nerve sheath tumors. Brain Pathol 2004;14:297–303. [PubMed: 15446585]
21. Mukhopadhyay D, Jung J, Murmu N, et al. CUGBP2 plays a critical role in apoptosis of breast cancer cells in response to genotoxic injury. Ann N Y Acad Sci 2003;1010:504–509. [PubMed: 15033780]
22. White FV, Anthony DC, Yunis EJ, et al. Nonrandom chromosomal gains in pilocytic astrocytomas of childhood. Hum Pathol 1995;26:979–986. [PubMed: 7672798]
23. Deshmukh H, Yeh TH, Yu J, et al. High-resolution, dual-platform aCGH analysis reveals frequent HIPK2 amplification and increased expression in pilocytic astrocytomas. Oncogene 2008;27:4745–4751. [PubMed: 18408760]
24. Jones DT, Ichimura K, Liu L, et al. Genomic analysis of pilocytic astrocytomas at 0.97 Mb resolution shows an increasing tendency toward chromosomal copy number change with age. J Neuropathol Exp Neurol 2006;65:1049–1058. [PubMed: 17086101]
25. Pfister S, Janzarik WG, Remke M, et al. BRAF gene duplication constitutes a mechanism of MAPK pathway activation in low-grade astrocytomas. J Clin Invest 2008;118:1739–1749. [PubMed: 18398503]
26. Bar EE, Lin A, Tihan T, et al. Frequent Gains at Chromosome 7q34 Involving BRAF in Pilocytic Astrocytoma. J Neuropathol Exp Neurol 2008;67:878–887. [PubMed: 18716556]
27. Sharma MK, Watson MA, Lyman M, et al. Matrilin-2 expression distinguishes clinically relevant subsets of pilocytic astrocytoma. Neurology 2006;66:127–130. [PubMed: 16401863]

28. Tanami H, Imoto I, Hirasawa A, et al. Involvement of overexpressed wild-type BRAF in the growth of malignant melanoma cell lines. Oncogene 2004;23:8796–8804. [PubMed: 15467732]
29. Kluwe L, Hagel C, Tatagiba M, et al. Loss of NF1 alleles distinguish sporadic from NF1-associated pilocytic astrocytomas. J Neuropathol Exp Neurol 2001;60:917–920. [PubMed: 11556548]
30. Dasgupta B, Li W, Perry A, et al. Glioma formation in neurofibromatosis 1 reflects preferential activation of K-RAS in astrocytes. Cancer Res 2005;65:236–245. [PubMed: 15665300]
31. Sharma MK, Zehnbauer BA, Watson MA, et al. RAS pathway activation and an oncogenic RAS mutation in sporadic pilocytic astrocytoma. Neurology 2005;65:1335–1336. [PubMed: 16247081]
32. Janzarik WG, Kratz CP, Loges NT, et al. Further evidence for a somatic KRAS mutation in a pilocytic astrocytoma. Neuropediatrics 2007;38:61–63. [PubMed: 17712732]
33. Natarajan G, Ramalingam S, Ramachandran I, et al. CUGBP2 downregulation by prostaglandin E2 protects colon cancer cells from radiation-induced mitotic catastrophe. Am J Physiol Gastrointest Liver Physiol 2008;294:G1235–G1244. [PubMed: 18325984]
34. Goldberg I, Davidson B, Reich R, et al. Alphav integrin expression is a novel marker of poor prognosis in advanced-stage ovarian carcinoma. Clin Cancer Res 2001;7:4073–4079. [PubMed: 11751504]
35. Nikkola J, Vihinen P, Vlaykova T, et al. Integrin chains beta1 and alphav as prognostic factors in human metastatic melanoma. Melanoma Res 2004;14:29–37. [PubMed: 15091191]
36. Lu JG, Sun YN, Wang C, et al. Role of the alphav-integrin subunit in cell proliferation, apoptosis and tumor metastasis of laryngeal and hypopharyngeal squamous cell carcinomas: a clinical and in vitro investigation. Eur Arch Otorhinolaryngol. 2008
37. Brendle A, Lei H, Brandt A, et al. Polymorphisms in predicted microRNA-binding sites in integrin genes and breast cancer: ITGB4 as prognostic marker. Carcinogenesis 2008;29:1394–1399. [PubMed: 18550570]
38. Lee SK, Kim MH, Cheong JY, et al. Integrin alpha V polymorphisms and haplotypes in a Korean population are associated with susceptibility to chronic hepatitis and hepatocellular carcinoma. Liver Int. 2008
39. Wang D, Li Z, Messing EM, et al. Activation of Ras/Erk pathway by a novel MET-interacting protein RanBPM. J Biol Chem 2002;277:36216–36222. [PubMed: 12147692]
40. Wang Y, Marion Schneider E, Li X, et al. HIPK2 associates with RanBPM. Biochem Biophys Res Commun 2002;297:148–153. [PubMed: 12220523]
41. Oleinik NV, Krupenko NI, Priest DG, et al. Cancer cells activate p53 in response to 10-formyltetrahydrofolate dehydrogenase expression. Biochem J 2005;391(Pt 3):503–511. [PubMed: 16014005]
42. Anthony TE, Heintz N. The folate metabolic enzyme ALDH1L1 is restricted to the midline of the early CNS, suggesting a role in human neural tube defects. J Comp Neurol 2007;500:368–383. [PubMed: 17111379]
43. Cahoy JD, Emery B, Kaushal A, et al. A transcriptome database for astrocytes, neurons, and oligodendrocytes: A new resource for understanding brain development and function. J Neurosci 2008;28:264–278. [PubMed: 18171944]
44. Krupenko SA, Oleinik NV. 10-formyltetrahydrofolate dehydrogenase, one of the major folate enzymes, is down-regulated in tumor tissues and possesses suppressor effects on cancer cells. Cell Growth Differ 2002;13:227–236. [PubMed: 12065246]
45. Pizzorno G, Moroson BA, Cashmore AR, et al. (6R)-5,10-Dideaza-5,6,7,8-tetrahydrofolic acid effects on nucleotide metabolism in CCRF-CEM human T-lymphoblast leukemia cells. Cancer Res 1991;51:2291–2295. [PubMed: 1707749]
46. Beardsley GP, Moroson BA, Taylor EC, et al. A new folate antimetabolite, 5,10-dideaza-5,6,7,8-tetrahydrofolate is a potent inhibitor of de novo purine synthesis. J Biol Chem 1989;264:328–333. [PubMed: 2909524]

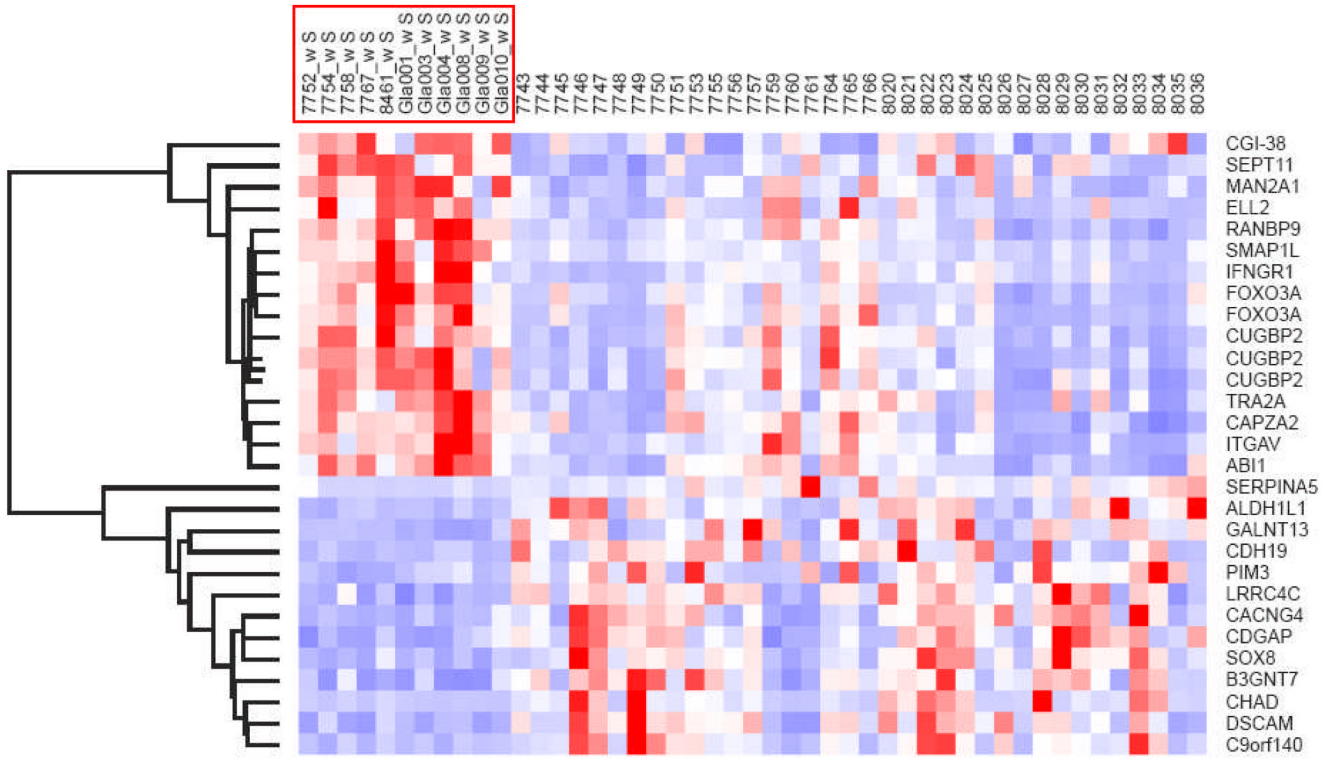

Figure 1.

NF1-associated pilocytic astrocytoma gene signature. The heat map represents the top candidate genes that were relatively over- or underexpressed in NF1-associated vs. sporadic pilocytic astrocytomas after unsupervised hierarchical clustering (NF1-associated samples are highlighted in the red box).

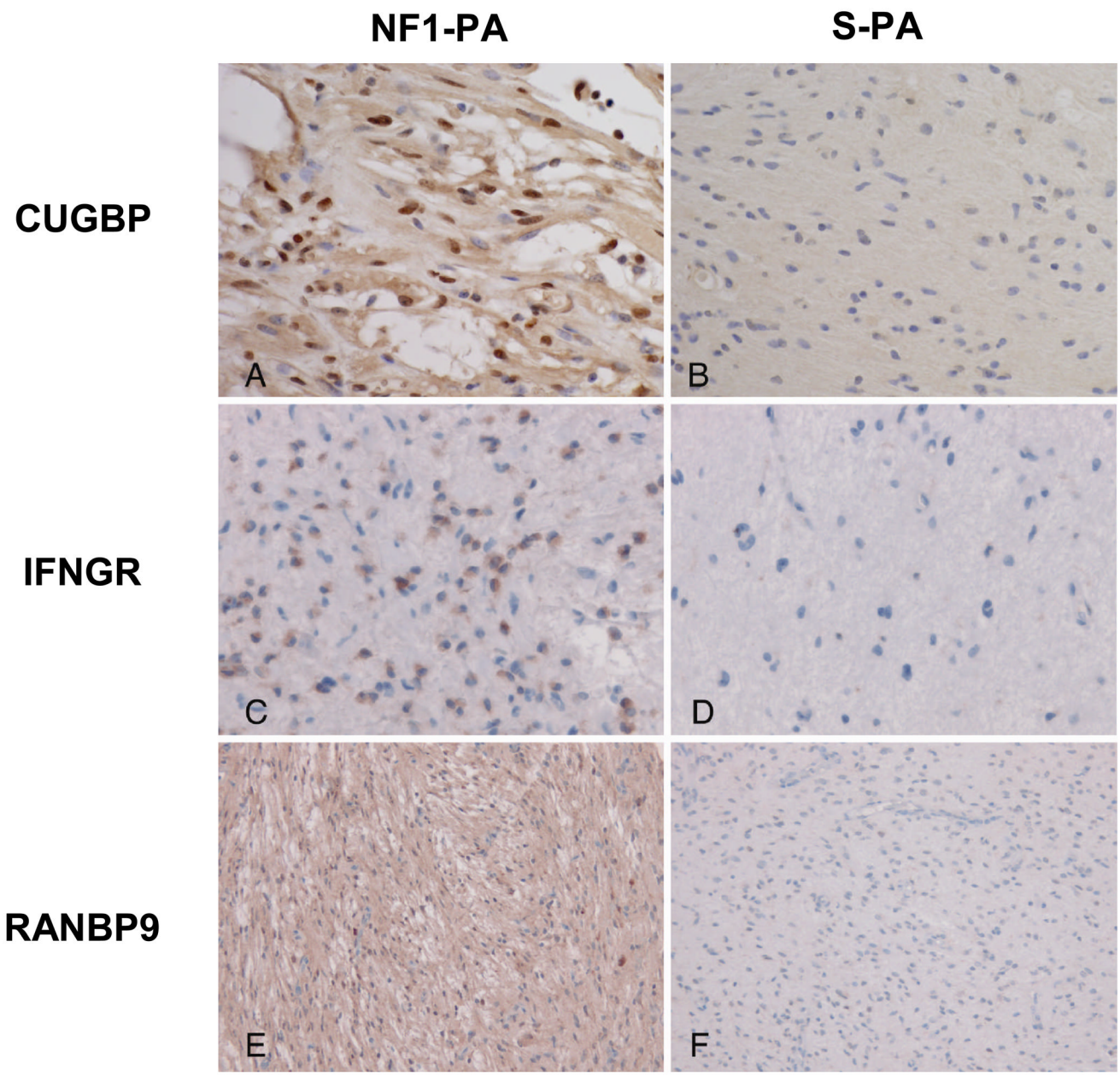

Figure 2.

Validation of NF1-associated pilocytic astrocytoma gene expression signature. Representative immunohistochemistry results for CUGBP (**A, B**), IFNGR (**C, D**), and RANBP9 (**E, F**) in TMA PA sections. Positive CUGBP staining is nuclear in **A**; IFNGR staining is cytoplasmic in **C**; RANBP9 staining is both nuclear and cytoplasmic in **E**. Immunostaining is greater for each in NF1-associated PAs (NF1-PA) (**A, C, E**) compared to sporadic PAs (S-PA)(**B, D, F**). Magnifications: A–D, 400x; E, F, 200x.

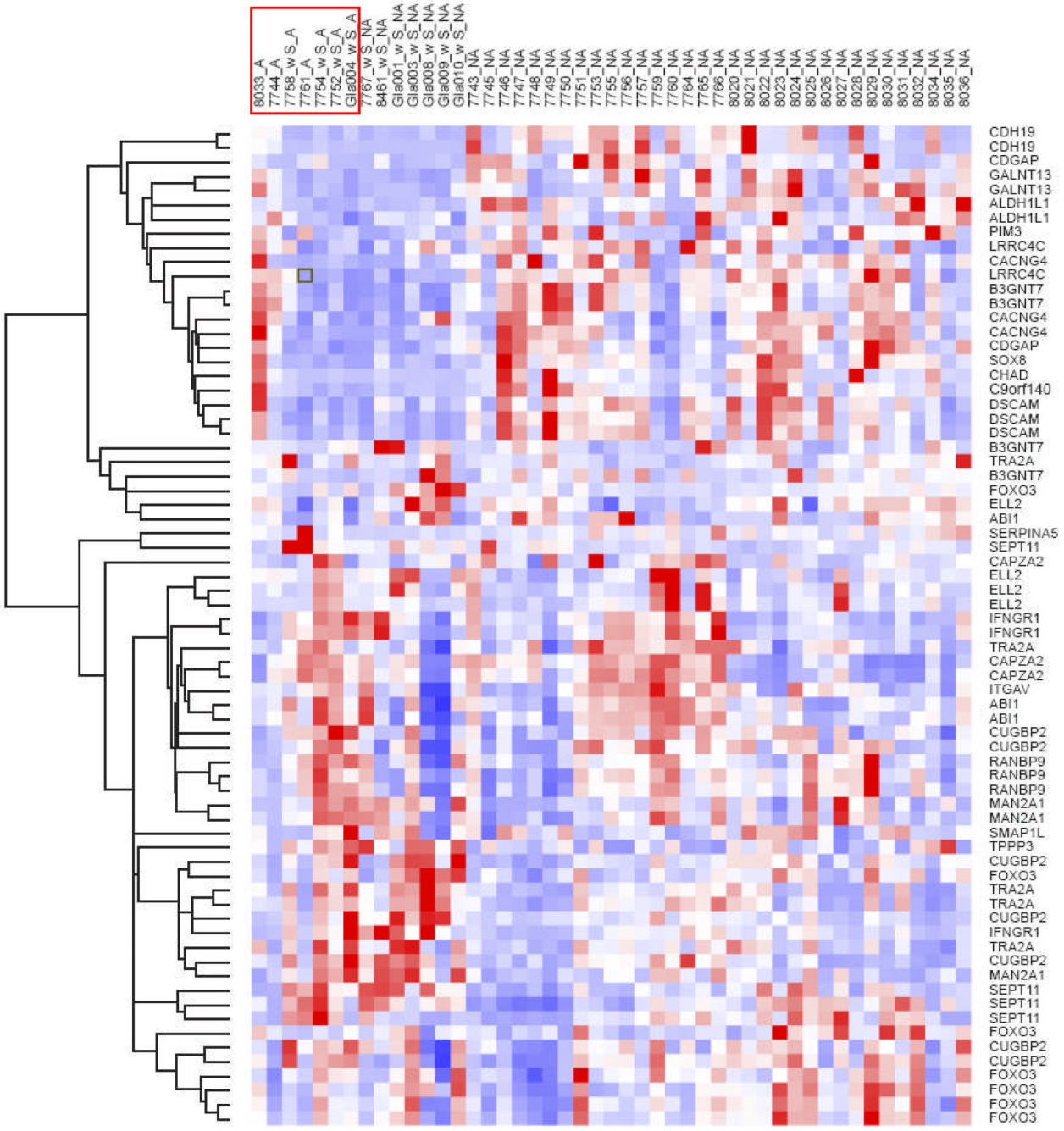

Figure 3.

Clustering of aggressive vs. typical PA using the list of genes identified in NF1-associated versus sporadic PA demonstrates no overall differences in gene expression between the two groups for most genes with the exception of 3 candidate genes that are relatively underexpressed in aggressive PA, i.e. ALDH1L1 ($p = 0.019$), SOX 8 ($p = 0.038$), CDGAP ($p = 0.04$) (Wilcoxon rank sum test). Aggressive PAs are highlighted in the red box.

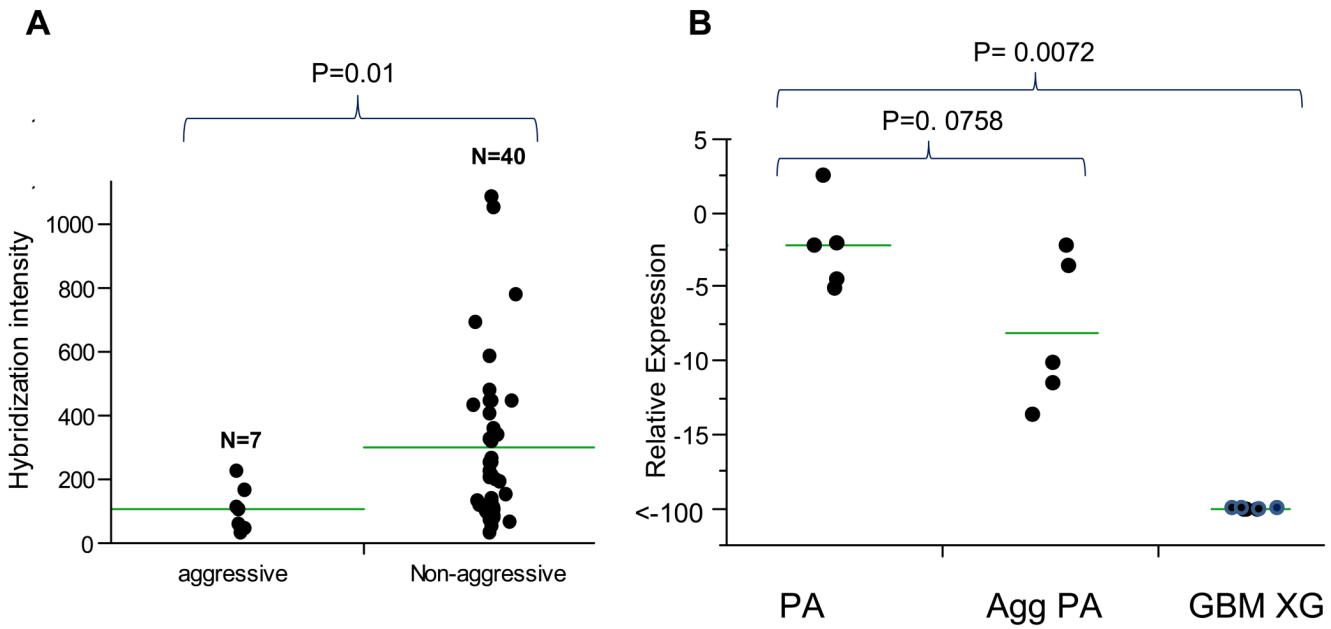

Figure 4.

ALDH1L1 RNA expression is decreased in aggressive (Agg PA) compared to typical PAs. Gene expression was measured using data from Affymetrix U133 Plus2.0 GeneChip arrays. (**A**) There is less hybridization intensity in aggressive PA (probe set 205208_at; p = 0.019). (**B**) Quantitative real time PCR demonstrated a stepwise decrease of ALDH1L1 expression as measured by fold change in aggressive PAs and heterotopic glioblastoma xenografts (GBM XG). (Wilcoxon rank-sum test) (horizontal bars = mean of each group).

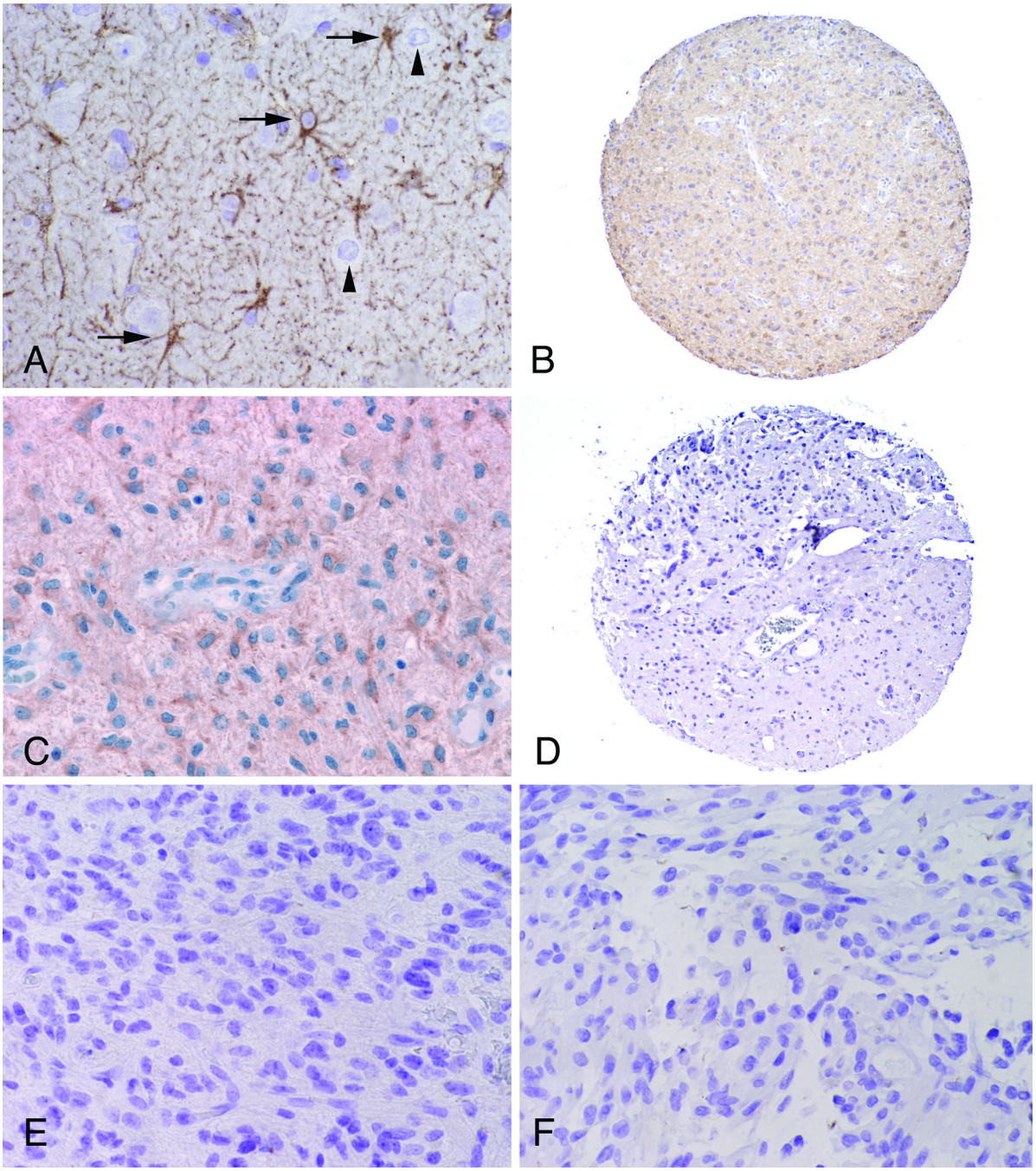

Figure 5.

ALDH1L1 protein is relatively underexpressed in aggressive PA. (**A**) A non-neoplastic seizure control illustrates ALDH1L1 strong expression in the body and cell processes of reactive astrocytes (arrows) but not in neurons (arrowheads). (**B, C**) Typical PAs with diffuse immunostaining for ALDH1L1. Intratumoral vessels are negative (**C**, center). (**D, E**) Clinically aggressive PA are negative for ALDH1L1, especially in cellular areas. (**F**) An example of the aggressive histologic variant pilomyxoid astrocytoma is also negative. Magnifications: A, C, E, F, 400x; B, D, 40x.

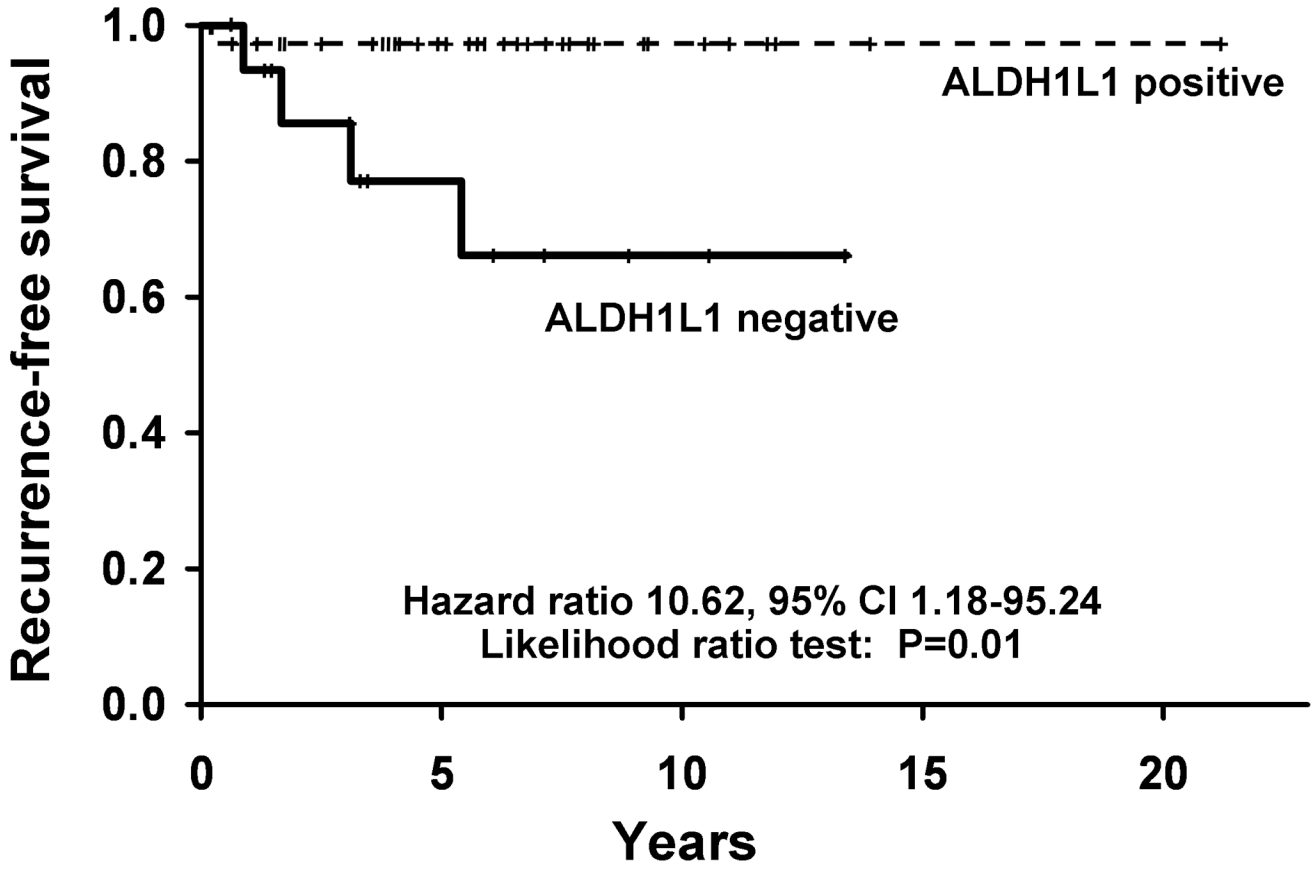

Figure 6.
Patients with ALDH1L1-immunonegative tumors exhibit decreased recurrence-free survival ($p = 0.01$).

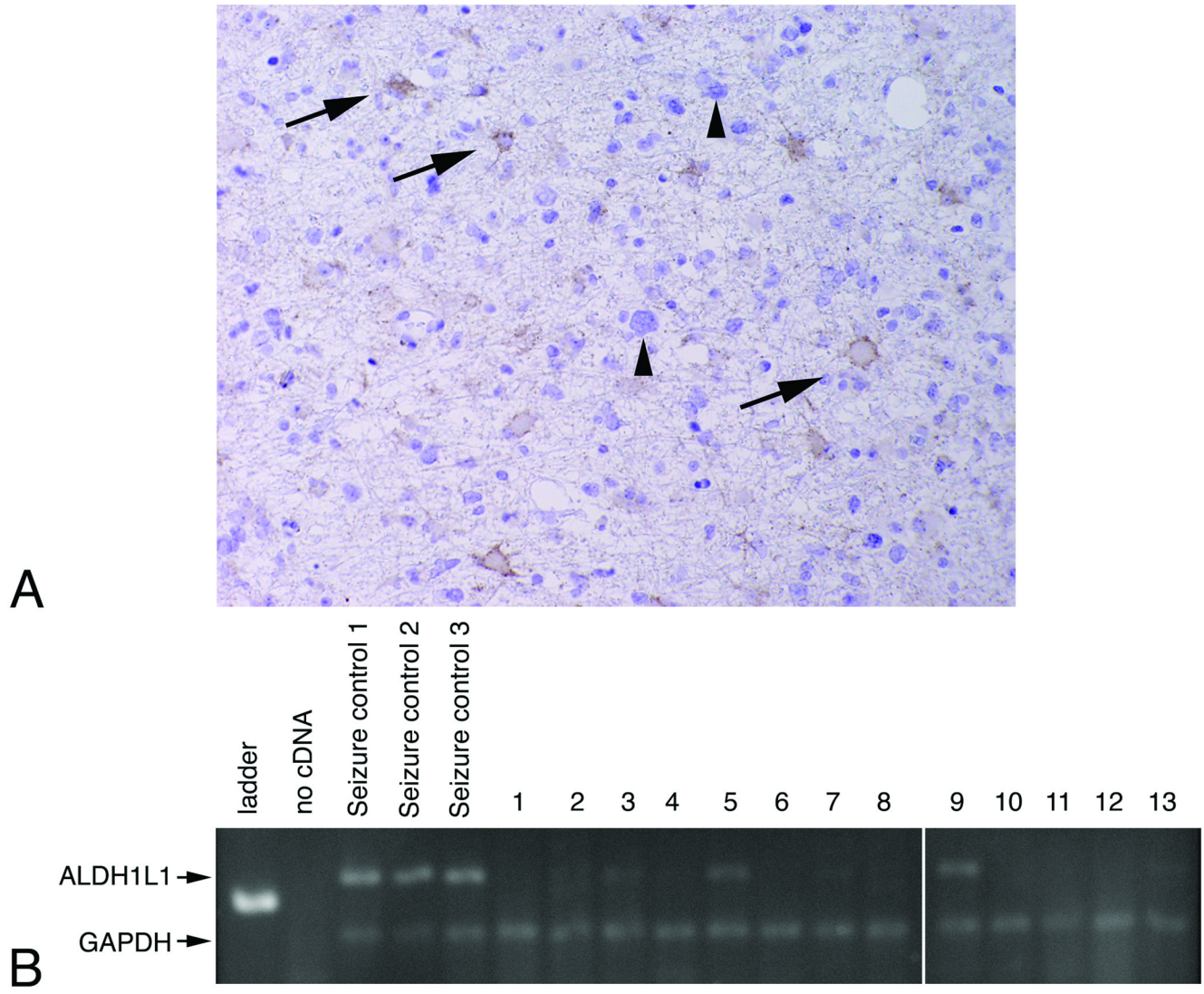

Figure 7.

ALDH1L1 expression is decreased in infiltrating astrocytomas. (**A**) ALDH1L1 immunoreactivity was not detected in cytologically atypical neoplastic astrocytes (arrowheads) but was found in entrapped reactive astrocytes (arrows) (Magnification: 400x). (**B**) Representative RT-PCR gel demonstrates decreased to absent *ALDH1L1* expression in glioblastoma heterotopic xenografts (lanes 1–13) compared to non-neoplastic gliosis (seizure control lanes 1–3) brain samples. *ALDH1L1* and *GAPDH 117* and 73 base pair products are demonstrated. All samples are from the same gel run and exposure.

Table 1

Antibodies Used for Immunohistochemical Studies

Antibody	Source	Clone	Dilution
ALDH1L1	Novus Biologicals, Littleton, CO	3E9	1:100
CUGBP2	Dr. Shrikant Anant; Oklahoma City, OK	rabbit polyclonal	1:200
IFNGR1	ProteinTech Group, Inc, Chicago, IL	rabbit polyclonal	1:100
RANBP9	ProteinTech Group, Inc.	rabbit polyclonal	1:25
FOXO3A	Lifespan Biosciences, Seattle, WA	rabbit polyclonal	1:250
PIM-3	Professor Naofumi Mukaida, Kanazawa University, Japan	rabbit polyclonal	1:100
ITGAV1	Abcam, Cambridge, MA	clone 272–17E6	1:100
ABI-1	MBL international corporation, Woburn, MA	clone 1B9	1:250
SERPINA5	ProteinTech Group, Inc.	rabbit polyclonal	1:100
COX-2	Dako	clone CX-294	1:50
Neurofilament protein	Dako	clone 2F11	1:800
Ki67	Dako	clone MIB-1	1:300

Table 2

Immunohistochemical Analysis of NF1-Associated Pilocytic Astrocytoma (PA)-Specific Gene Expression

	Pilocytic astrocytoma		
Protein staining pattern	**NF1-Associated**[1]	**Sporadic**[1]	**p value**[2]
CUGBP2 strong nuclear	3/13 (23)	0/34 (0)	0.001
RANBP9 nuclear and cytoplasmic	8/14 (57)	19/77(25)	0.008
ITGAV cytoplasmic	10/14 (71)	13/65 (20)	0.0001
INFGR1 cytoplasmic	10/12 (83)	28/73 (38)	0.024
ABI1 cytoplasmic	6/15 (40)	14/71 (20)	0.058
FOXO3A nuclear only cytoplasmic only	3/13 (23) 6/13 (46)	9/73 (12) 16/73 (22)	0.180 0.474
ALDH1L1 cytoplasmic	5/9 (56)	34/48 (71)	0.839
SERPINA5 cytoplasmic	4/13 (31)	32/72 (44)	0.494
PIM3 cytoplasmic	10/12 (83)	43/57 (75)	0.581

[1] Number of positive cases/number of cases tested (% positive).

[2] Regression analyses was performed after adjusting for tumor location.

Table 3

Genes Underexpressed in Aggressive (n = 7) Compared to Non-aggressive (n = 40) PAs

Probe_set	UniGene ID	Gene Title	Gene Symbol	Fold Change (non-aggressive/aggressive)	p value[1]
205208_at	Hs.434435	aldehyde dehydrogenase 1 family, member L1	ALDH1L1	3.35	0.019
226913_s_at	Hs.243678	SRY (sex determining region Y)-box 8	SOX8	3.18	0.038
226056_at	Hs.477278	Cdc42 GTPase-activating protein	CDGAP	1.91	0.040

[1]Wilcoxon Rank-Sum Test

Table 4

ALDH1L1 Expression Correlates with Glial Tumor Clinical Behavior

Tumor	Total number of tumors[1]	Positive[2]
Pilocytic astrocytoma		
Typical[3]	46	36 (78)
Aggressive/recurrent[4]	24	6 (25)
With pilomyxoid features	9	1 (11)
With anaplastic transformation	10	3 (30)
Infiltrating astrocytoma	21	5 (24)
Seizure brain controls	3	3 (100)

[1] Number of cases tested.

[2] Number of positive cases (% positive).

[3] Staining performed on TMA sections.

[4] Staining performed on both TMA (n = 6) and full sections (n = 18).